Experimental Brain Research (2022) 240:2907–2921
https://doi.org/10.1007/s00221-022-06463-y

RESEARCH ARTICLE

The effect of doxorubicin or cyclophosphamide treatment on auditory brainstem response in mice

Maxwell Hennings[1] · **Thane Fremouw**[2,3]

Received: 9 April 2022 / Accepted: 7 September 2022 / Published online: 19 September 2022

Abstract

Clinical studies suggest that chemotherapy is associated with long-term cognitive impairment in some patients. Several underlying mechanisms have been proposed; however, the etiology of chemotherapy-related cognitive dysfunction remains relatively unknown. There is evidence that oligodendrocytes and white matter tracts within the CNS may be particularly vulnerable to chemotherapy-related damage and dysfunction. Auditory brainstem responses (ABRs) have been used to detect and measure functional integrity of myelin in a variety of animal models of autoimmune disorders and demyelinating diseases. Limited evidence suggests that increases in interpeak latencies, associated with disrupted impulse conduction, can be detected in ABRs following 5-fluorouracil administration in mice. It is unknown if similar functional disruptions can be detected following treatment with other chemotherapeutic compounds and the extent to which alterations in ABR signals represent robust and long-lasting impairments associated with chemotherapy-related cognitive impairment. Thus, C57BL/6 J mice were treated every 3rd day for a total of 3 injections with low or high dose cyclophosphamide, or doxorubicin. ABRs of mice were assessed on days 1, 7, 14, 56 and 6 months following completion of chemotherapy administration. There were timing and amplitude differences in the ABRs of the doxorubicin and the high dose cyclophosphamide groups relative to the control animals. However, despite significant toxic effects as assessed by weight loss, the changes in the ABR were transient.

Keywords Cyclophosphamide · Doxorubicin · Auditory brainstem response · ABR · Myelin · Chemo-brain · Chemo-fog · Cancer-related cognitive impairment · Chemotherapy-related cognitive impairment · CRCI · Chemotherapy-induced cognitive impairment · CICI

Introduction

Cancer patients treated with adjuvant chemotherapy often experience cognitive decline. This phenomenon, often dubbed "Chemo-Brain," or "Chemo-Fog" can be long lasting (> 10 years) and can severely impact the survivor's quality of life (Raffa and Tallarida 2010). It is estimated that as of January 1, 2019, 67% of cancer survivors (10.3 million) in the US were diagnosed 5 or more years ago, demonstrating the success of chemotherapy and other treatments for cancer (Miller et al. 2019). Unfortunately, this also means there is a growing population of survivors who struggle with long-term problems in mental function, formally referred to as chemotherapy-related cognitive impairment (CRCI). These long-lasting cognitive impairments following chemotherapy treatment are known to occur across a diverse range of processes including working memory, attention, processing speed, concentration, and executive functions (Collins et al. 2014; Janelsins et al. 2018; Koppelmans et al. 2012; for a recent review see: Cerulla et al. 2020) .

The cause of these cognitive impairments and the extent to which chemotherapy treatment itself may be responsible for cognitive dysfunction detected in cancer survivors remains unclear. Methodological limitations such as lack of baseline measurements, variation in the neuropsychological assessments used, relatively small sample sizes, and variations in anti-cancer treatment intensity and type complicate

Communicated by Bill J Yates.

✉ Maxwell Hennings
henningsma@longwood.edu

[1] Department of Psychology, Longwood University, Farmville, VA, USA

[2] Department of Psychology, University of Maine, Orono, ME, USA

[3] Graduate School of Biomedical Science and Engineering, University of Maine, Orono, ME, USA

studies in humans (Evenden 2013; Vardy et al. 2007; Wefel et al. 2011; Winocur et al. 2018). These limitations, coupled with inherent interactions between genetics, epigenetic, and environmental factors present in clinical populations, create large sources of variance in collected data. As a result of these confounds, researchers have expressed the need for better methodologies and the development of animal models that allow for more exacting experimental control and better synergies between animal models and human experiments (Weiss 2010; Winocur et al. 2018). We and others have begun to develop animal models of chemotherapy induced cognitive decline to investigate the underlying neural mechanisms and complement continued human research (e.g., Briones and Woods 2011; Christie et al. 2012; Foley et al. 2008; Fremouw et al. 2012a, 2012b; Gandal et al. 2008; Janelsins et al. 2010; Long et al. 2011; MacLeod et al. 2007; Matsos and Johnston 2019; Reiriz et al. 2006; Seigers and Fardell 2011; Winocur et al. 2012; Wood et al. 2006).

The neural targets and physiological mechanisms related to cognitive dysfunction following chemotherapy are likely complicated and varied (Ahles and Saykin 2007; Ren et al. 2019). One possible underlying mechanism is damage and disruption to white matter within the CNS. Clinical studies suggest white matter pathology following chemotherapy treatment is common, regardless of chemotherapy regimen or cancer type (Matsos et al. 2017). The extent to which these changes in white matter persist is less clear, but for some, recovery from chemotherapy-induced changes to white matter occurs within 3–4 years after treatment (Billiet et al. 2018). In vitro and in vivo experimentation has found that at least some chemotherapy agents can be toxic to both oligodendrocyte precursor cells as well as mature oligodendrocytes, resulting in long term damage to myelin tracts in the CNS (Han et al. 2008). Furthermore Geraghty et al. (2019) found that chemotherapy treatment with methotrexate disrupts activity-regulated myelination in a mouse model of CRCI. Therefore, myelin disruption may be one of the causes of observed cognitive impairment in clinical populations receiving chemotherapy, and as such, auditory brainstem response (ABR) analysis may be a useful tool for identifying this damage.

The ABR is a relatively robust and early event-related potential that has an established history for the assessment of hearing and the integrity of auditory nerve (Martin et al. 2007; Jerger and Hall 1980; Zheng et al. 1999). Utilizing ABRs, electrodes can detect evoked electrical potentials at various stages along the initial auditory pathway, with peaks representing processing along the auditory pathway from the cochlea through the midbrain (Henry 1979; Land et al. 2016; Long et al. 2018). The noninvasive nature of ABR recording, and its relative insensitivity to subject state, make it an attractive assessment technique in both clinical and research settings for studying disorders of the CNS, including myelin damage (Parham et al. 2001; Shah and Salamy 1980). Moreover, ABRs are easily measured in both humans and non-human animals. Myelin deficiency causes changes in electrophysiological features of neurons because of decreased conduction velocity, prolonged refractory periods, desynchronized firing and increased membrane time constants (Brismar 1981; Cragg and Thomas 1964). These electrophysiological changes can be detected with ABR analysis and have been studied in several mutant animal models of abnormal myelin development and demyelination (Carpinelli et al. 2014; Naito et al. 1999; Roncagliolo et al. 2000; Shah and Salamy 1980; Wan and Corfas 2017; Zhou et al. 1995). The exact nature of the changes to the ABR differ in the different models of myelin damage; however, there is typically a decrease in various interpeak latencies (often P1 to P5 or P1 to P4 is measured) and a decrease in amplitude at various peaks. The specific peaks for which amplitude decreases vary, likely based on the nature of the myelin damage including if it is peripheral, central, or both.

Han et al. (2008) found that mice treated with the chemotherapy agent 5-fluorouracil (5-FU) had increased ABR interpeak latencies indicative of myelin damage. Interestingly, the increase in ABR interpeak latency developed over time, suggesting delayed white matter damage which was confirmed in a follow-up experiment in which they found reduced cellularity and loss of myelin basic protein in the corpus callosum in mice at 6-month post-5-FU treatment. Thus, myelin in the CNS may be damaged by chemotherapeutic agents, and ABR analysis may be a useful tool for identifying such damage.

If ABR recordings are sensitive to damage related to chemotherapeutic agents (myelin or otherwise), the ease of diagnostic application in clinical settings, the relative robust nature of the ABR signal, and the similarities between rodent and human applications would make ABRs a useful tool for identifying early signs of cognitive sequelae (Ogier 2020), for identifying individuals that may be at risk for developing CRCI, and for helping to reconcile the animal and human research literature.

To further investigate this phenomenon, we conducted a study designed to examine the effects of the chemotherapy agents cyclophosphamide and doxorubicin on the ABRs of mice. We hypothesized that mice treated with cyclophosphamide or doxorubicin would exhibit abnormal ABRs when compared to saline treated control animals. Specifically, we expected to observe increases in the interpeak latency between P1 and P5 and decreases in at least some peak amplitudes that relate to myelin damage, reduced impulse conduction, and desynchronized neural firing.

Experimental procedure

General

Thirty-nine male C57BL/6 J mice were obtained from Jackson Laboratories (Bar Harbor, ME) at 8–9 weeks of age. Mice were housed 3–4 animals per cage with food and water provided ad libitum. A 12:12 light dark cycle was used (light on: 7:30 am–7:30 pm). Experiments started 2 weeks after arrival of the animals according to the protocol described below. All experiments were approved by the Institutional Animal Care and Use Committee (IACUC) at the University of Maine.

Following a 14-day acclimation period, mice received 3 intraperitoneal injections of saline (0.9% sterile saline, $n = 14$), doxorubicin (5 mg/kg dissolved in saline, $n = 8$), low dose cyclophosphamide (120 mg/kg dissolved in saline, $n = 8$), or high dose cyclophosphamide (220 mg/kg dissolved in saline, $n = 9$) with 2 days between injections. Intraperitoneal injections rather than intravenous injections were used to match the injection method employed in the rat and mouse CRCI literature. Dosing levels for the doxorubicin and high dose cyclophosphamide were based on dosing studies in our lab. Our goal was to use the highest dose that did not (1) lead to systemic animal death and (2) lead to permanent weight loss. Because toxicity and tolerance of cancer chemotherapy agents can vary drastically as a function of circadian rhythm (Focan 1995), we treated all mice at approximately the same time: 8 h after light onset. This difference in toxicity and tolerance based on circadian rhythm can make comparing dosing across studies difficult if the time of dosing is not listed. Starting 2 days before treatment, and continuing 14 days after the last drug treatment, the mice were weighed daily. Thereafter, mice were weighed at least every third day.

An initial baseline ABR recording (day 0) was carried out 48 h before animals received their first chemotherapy injection. ABR recording sessions were repeated a total of five additional times: on days 1, 7, 14, 56, and 6 months following completion of chemotherapy administration. Figure 1 shows the timeline of the experiment.

ABR stimuli and recording procedure

ABR recordings were carried out in a double-walled sound attenuating chamber (Industrial Acoustics) under ketamine/xylazine anesthesia (100 mg/kg ketamine; 10 mg/kg xylazine). The anesthesia was used to immobilize the mice and allow for artifact free recordings. A heating pad (FHC) regulated by a temperature probe was used to keep the mouse warm (36 °C) during the ABR procedure.

ABRs were recorded using metal subdermal electrodes (Technomed) connected to a Tucker–Davis Technologies (TDT) RA4LI low impedance headstage. The active electrode was placed subcutaneously at the vertex. The reference electrode was placed subcutaneously ventral lateral to the left external pinna. A ground electrode was placed subcutaneously near the tail. The evoked signals were amplified and digitized via a TDT RA4PA preamplifier, acquired with a TDT RX5-2 Pentusa Bases Station running at a sampling rate of 25 K, and bandpass filtered (150–3000 Hz). ABRs were elicited with a series of free-field, 100 µs square-wave clicks presented at a rate of 20 clicks per second via a TDT MF1 speaker. The speaker was in front of the mouse, 12.5 cm from the middle of its head. Clicks were digitally generated and converted to an analog signal via a TDT RX6 running at a sampling rate of 200 K. Clicks were presented over 12 trials from 90 to 30 dB pSPL in 5 dB steps. The speaker was calibrated (Burkard 2006) with an ACO Pacific 7016 ¼—in condenser microphone, 4016 preamplifier, 9200 power supply, and a TDT MA3 microphone amplifier. Each trial consisted of 500 individual stimulus presentations at a

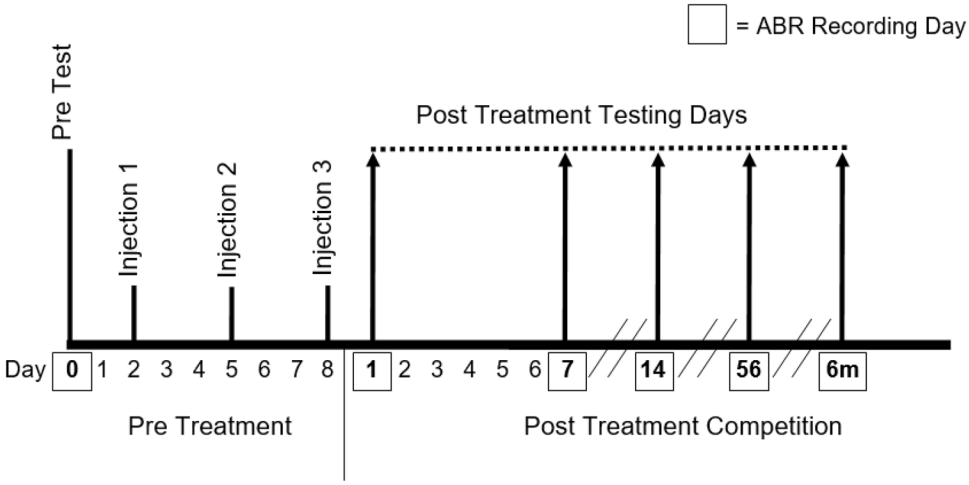

Fig. 1 Timeline. Initial baseline ABR recordings were performed 2 days prior to initial chemotherapy administration. Chemotherapy administration consisted of 3 i.p. injections administered every third day. Follow-up ABR recordings were performed on days 1, 7, 14, 56 and 6 months following completion of chemotherapy administration

single sound level. All recordings and stimuli presentations were programmed and controlled via Tucker Davis Technologies' System3 Bio-SigRP© software. After the ABR recordings were concluded, mice were placed in an externally heated empty cage and allowed to recover before being returned to their home cage.

Data analysis

After ABR recordings were completed, data were exported to MATLAB for analysis. Blocks of 500 individual responses for each animal for each trial were averaged. Artifact rejection and peak/trough identification was automated via custom MATLAB programs and then checked by eye by two observers with the observers blind to treatment. When checking by eye, an animal's averaged waveforms were stacked by sound level (see Fig. 2) to aid in identification of the peaks and troughs. Identification of P2 can be complicated by multiple peaks within close temporal and amplitude proximity. The blind observers did modify the P2 and corresponding trough location for a few animals on a few days. This was done in cases, where

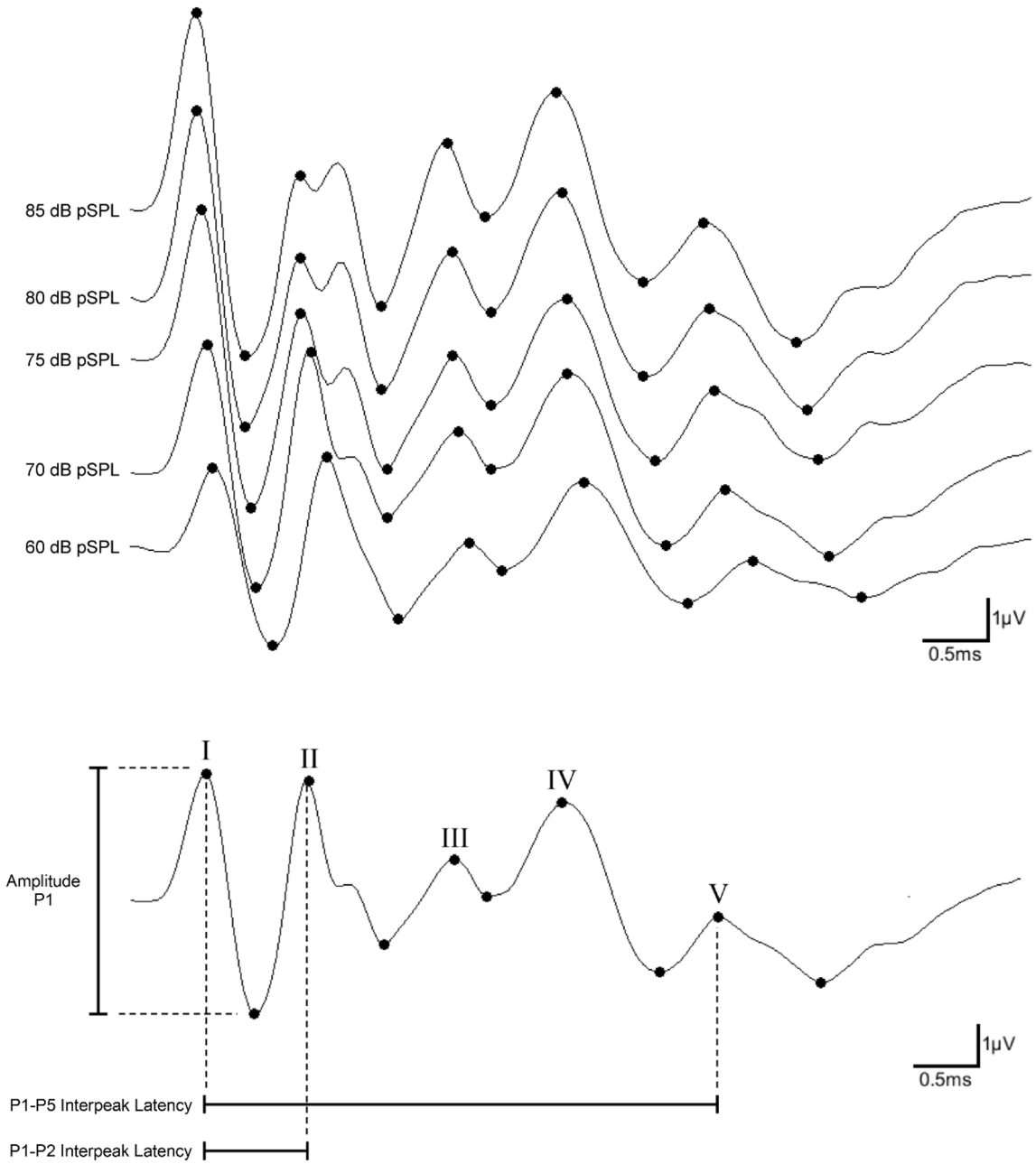

Fig. 2 Example of ABR waveforms stacked by sound level with peaks and troughs marked

one of the distinct peaks was lower in amplitude than the other peak and it was clear that that lower amplitude peak corresponded to the peak at lower sound levels. An example of this is shown in Fig. 2. At 85 dB pSPL, there are two peaks, the second of which is higher in amplitude. Although the second peak is higher in amplitude, the first peak clearly corresponded to P2 at lower sound levels and was, therefore, labeled as P2. The same approach was used in determining the corresponding trough, as shown in Fig. 2.

Changes in interpeak latency were analyzed for each mouse, calculated as L_t–$L_{0,}$ where L_t is the interpeak latency [time between the corresponding 2 peaks] at day 1, day 7, day 14, day 56, or 6-month post-treatment, and L_0 is the baseline interpeak latency 2 days prior to the initial i.p. injection, day 0. Positive values on this measure indicate a slower recorded interpeak latency during a specific follow-up ABR recording relative to baseline. Negative values on this measure indicate a faster recorded interpeak latency during a specific follow-up ABR recording relative to baseline. Changes in peak amplitude were analyzed for each mouse, calculated as A_t–$A_{0,}$ where A_t is the amplitude [peak to following trough] at day 1, day 7, day 14, day 56, or 6-month post-treatment, and A_0 is the baseline amplitude 2 days prior to the initial i.p. injection, day 0. Threshold was determined as the minimum stimulus intensity that caused a reliable wave (I, II, III IV or V) by eye by two raters blind to treatment.

The most robust data were observed between 60 and 80 dB pSPL. As a result, longitudinal analyses were conducted with mixed model ANOVAs utilizing data recorded with stimuli presented at 60, 70, and 80 dB pSPL.

Results

Weight loss

Figure 3 depicts mean percent weight as a function of day, starting from the day of the first injection to the final injection, including every subsequent ABR recording day during the experiment (1, 7, 14, 56 and 6 months). As shown in Fig. 3, all animals injected with a chemotherapy agent, regardless of dose or specific compound, initially lost weight, while control animals receiving saline increased in weight.

To assess differences in the extent of weight lost between the treatment groups across the protocol, a two-factor mixed-design ANOVA [Treatment × Time] was conducted to analyze weight loss for the first 7 days (starting from the day of the first injection to the final injection) and every subsequent ABR recording day during the experiment (1, 7, 14, 56 and 6 months). The analysis indicated main effects of treatment, ($F_{3,\ 35} = 50.022$; $p < 0.001$, $\eta_p^2 = 0.811$), and time, ($F_{2.2,\ 76.7} = 118.942$; $p < 0.001$, $\eta_p^2 = 0.773$, Greenhouse–Geisser corrected), as well as a significant treatment by time interaction, ($F_{6.6,\ 76.7} = 14.448$; $p < 0.001$, $\eta_p^2 = 0.553$, Greenhouse–Geisser corrected).

Simple effect analyses utilizing ANOVAs at each timepoint assessed the interaction between treatment and time which revealed significant effects of treatment on weight loss at each timepoint (p's < 0.001). By day 1, all chemotherapy treated groups had lost significantly more weight than saline treated controls (pairwise comparisons using Fisher's LSD indicated p's < 0.01). These differences compared to controls remained at day 7 (p's < 0.01). By day 14

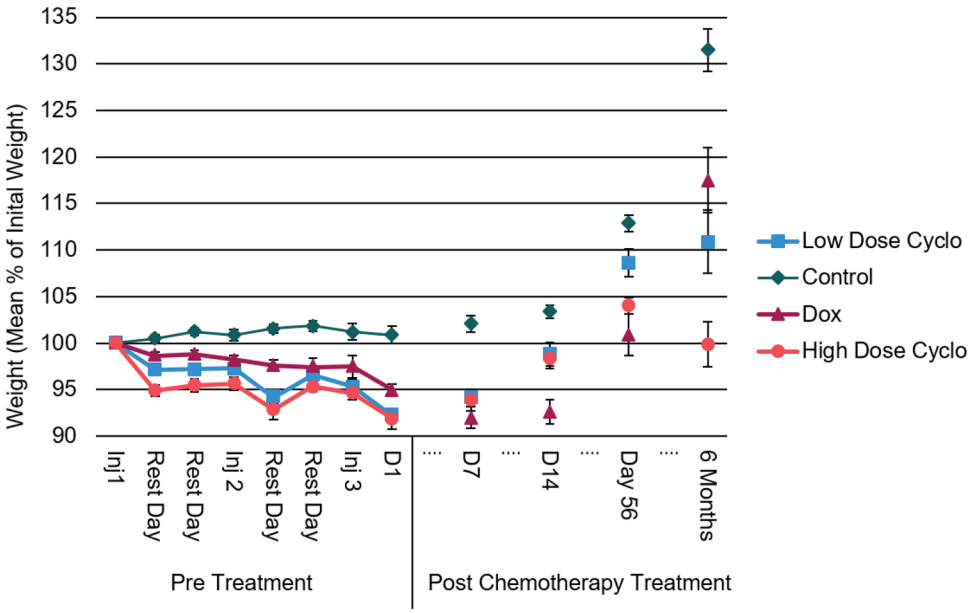

Fig. 3 Mean % body weight (relative to pre-treatment weight) as a function of day. A two-factor mixed-design ANOVA indicated a main effect of treatment, a main effect of time and a treatment by time interaction (all p's < 0.001) Error bars represent ± S.E.M

cyclophosphamide treated animals had nearly recovered to pre-injection weights; however, all chemotherapy groups remained significantly lighter than the control animals (p's < 0.01). By day 56 all chemotherapy groups had recovered to pre-injection weights; however, all chemotherapy groups were significantly lighter than the control animals, which was also the case at 6 months (p's < 0.01). These results suggest that chemotherapy dosing had an effect on weight and that control animals increased their weight over the protocol, while animals injected with either cyclophosphamide or doxorubicin initially lost weight, and then eventually recovered this weight. However, their weight was always less than control animals.

ABR auditory threshold

To determine if there were any difference in auditory threshold between the treatment groups across the protocol, a two-factor mixed-design ANOVA [Treatment × Time] was conducted to analyze change in threshold across each ABR recording day relative to baseline threshold. The analysis indicated a significant main effect of Time, ($F_{3.4,\ 118.9} = 13.31$; $p < 0.001$, $\eta_p^2 = 0.276$, Greenhouse–Geisser corrected), but there was no significant main effect of treatment, ($F_{3,\ 35} = 0.12$; $p = 0.95$, $\eta_p^2 = 0.011$), and no significant treatment by time interaction, ($F_{10.2,\ 118.9} = 0.53$; $p = 0.87$, $\eta_p^2 = 0.044$, Greenhouse–Geisser corrected).

Follow-up pairwise comparison using Fisher's LSD to investigate the significant main effect of time confirmed that threshold change was significantly greater at 6 months compared to all other timepoints (p's < 0.001). The change in threshold at day 56 was significantly greater than at days 1 and 7 (p's < 0.01). These results suggest, as expected, that animals experienced age-related hearing loss over the 6-month protocol (particularly by 6 months). Table 1 shows threshold for each treatment group at each recording day.

ABR peak and interpeak latencies

Figure 4 shows the change in P1 latency and in interpeak latency (P1–P5, P1–P2, P2–P3, P3–P4, P4–P5) relative to baseline ABR recordings, across the experiment averaged across sound level (60, 70, and 80 dB pSPL).

Change in P1–P5 interpeak latency

To explore potential differences in peripheral and central transmission speed among the treatment groups, we initially examined change in P1–P5 interpeak latency (change relative to the baseline recording on day 0) with a three-factor mixed-design ANOVA [Treatment × Time × Sound Level] with treatment as a between-subjects factor, and time (days 1, 7, 14, 56, and 6 months) and sound level (60, 70, and 80 dB pSPL) as within-subjects factors. Results indicated a significant main effect of treatment ($F_{3,\ 35} = 5.650$; $p = 0.003$, $\eta_p^2 = 0.326$), of time ($F_{4,\ 140} = 6.098$; $p < 0.001$, $\eta_p^2 = 0.148$) and of sound level ($F_{1.4,\ 48.3} = 8.095$; $p = 0.003$, $\eta_p^2 = 0.188$, Greenhouse–Geisser corrected). The main effect of time and the main effect of treatment was qualified by a significant interaction between the two ($F_{12,\ 140} = 2.677$; $p = 0.003$, $\eta_p^2 = 0.187$).

Follow-up pairwise comparisons utilizing Fisher's LSD of the main effect of sound level indicated that the change in P1–P5 interpeak latency tended to become smaller as the sound level increased. Overall, the interpeak latency change was greater at 60 dB than at 70 dB or 80 dB pSPL (p's < 0.005) and there was a trend of the change in interpeak latency being greater at 70 dB than at 80 dB pSPL ($p = 0.053$).

Given that there was a time by treatment interaction and no time by treatment by sound level interaction, data were collapsed across sound level (see Fig. 4a). Simple effect analysis of the interaction between treatment and time revealed a significant difference in P1–P5 interpeak latency among the treatment groups on day 1 ($F_{3,\ 35} = 3.971$; $p = 0.015$, $\eta_p^2 = 0.254$), day 7 ($F_{3,\ 35} = 13.540$; $p < 0.001$, $\eta_p^2 = 0.537$), and day 14 ($F_{3,\ 35} = 5.793$; $p = 0.003$, $\eta_p^2 = 0.332$). Follow-up pairwise comparisons utilizing Fisher's LSD indicated that the high dose cyclophosphamide group had a significant increase in P1–P5 interpeak latency compared to both the control group and the low dose cyclophosphamide group on day 1 (p's < 0.008). At day 7, both the high dose cyclophosphamide and doxorubicin groups had significantly increased P1–P5 interpeak latency compared to the low dose cyclophosphamide group and the control group (p's < 0.03). In addition, the high dose cyclophosphamide group had a significantly greater increase in P1–P5 interpeak latency compared to the doxorubicin treated animals ($p = 0.033$). At day

Table 1 Threshold (dB pSPL)

Treatment	Day 0	Day 1	Day 7	Day 14	Day 56	6 Months
Control	38.9 ± 0.77	39.3 ± 0.089	39.6 ± 0.63	40.0 ± 0.52	40.7 ± 1.03	45.7 ± 1.27
Doxorubicin	40.0 ± 0.94	38.7 ± 0.82	40.6 ± 1.13	39.4 ± 0.62	40.6 ± 0.62	45.0 ± 1.34
High Cyclophosphamide	38.3 ± 1.28	38.9 ± 0.73	39.4 ± 1.00	40.6 ± 1.00	41.1 ± 0.73	43.3 ± 0.83
Low Cyclophosphamide	39.4 ± 1.13	40.6 ± 1.13	40.6 ± 1.13	40.0 ± 0.00	41.3 ± 0.81	46.3 ± 1.57

Means ± S.E.M

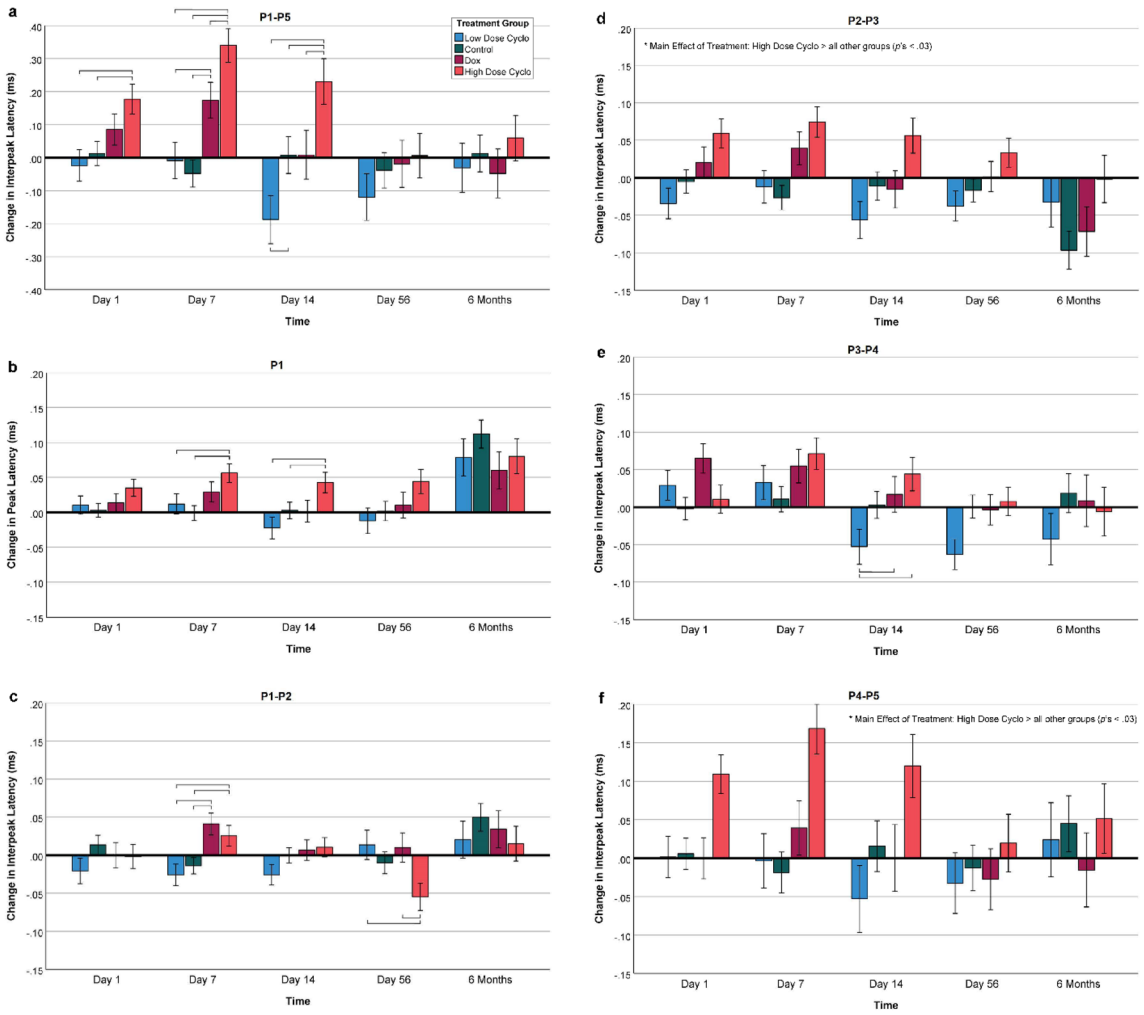

Fig. 4 Mean change in peak and interpeak latency from baseline. Baseline ABR recordings were performed for each animal 2 days before initiation of chemotherapy administration. After completion of chemotherapy administration, follow-up ABR tests were conducted on each animal at various points during a time course of 6 months. Low dose cyclophosphamide (120 mg/kg) and doxorubicin (5 mg/kg) both consisted of $n=8$ animals, the high dose cyclophosphamide (220 mg/kg) treatment group consisted of $n=9$ animals, and the control group consisted of $n=14$ animals. ABR latencies were analyzed for each individual at each timepoint. Change of peak or interpeak latency was calculated as L_t–L_0 (L_t, latency values at day 1, day 7, day 14, day 56, or 6-month post-treatment; L_0, baseline values 2 days before initiation of chemotherapy administration). The mean change in latency values were averaged across sound level (60, 70, and 80 dB pSPL) for **a** P1–P5, **b** P1, **c** P1–P2, **d** P2–P3, **e** P3–P4, **f** P4–P5. Data represent mean change of latency (ms) ± S.E.M. Brackets represent significant (p's < 0.05) Fisher's LSD pairwise comparisons. For P2–P3 and P4–P5, there was a significant overall difference between the high cyclophosphamide and all other groups (p's < 0.03)

14, the high dose cyclophosphamide treatment group had a significant increase in P1–P5 interpeak latency compared to all other treatment groups (p's < 0.04). In addition, the low dose cyclophosphamide treated animals had a significant decrease in P1–P5 interpeak latency compared to the control group ($p=0.041$).

Figure 5a shows mean ABR waveforms for each treatment group at day 0 and day 7 (averaged over sound level) and Fig. 5b, shows individual waveforms for two random animals from each group, also at day 0 and day 7 (averaged over sound level). These waveforms provide a visual example of some of the changes to P1–P5 interpeak latency noted above as well as some of the latency changes noted in other parts of "ABR peak and interpeak latencies" and some of the amplitude changes noted in "ABR peak amplitude". The mean group waveforms for both high dose cyclophosphamide and doxorubicin groups appear shifted to the right at day 7 compared to baseline recordings at day 0 and represent a slowing of the ABR signal. These same patterns are seen in the individual waveforms, in which the animals treated with high dose cyclophosphamide show both increased peak latency and decreased amplitude at some peaks. These patterns are most evident when viewing the high dose cyclophosphamide treated animals, but can be detected in the doxorubicin

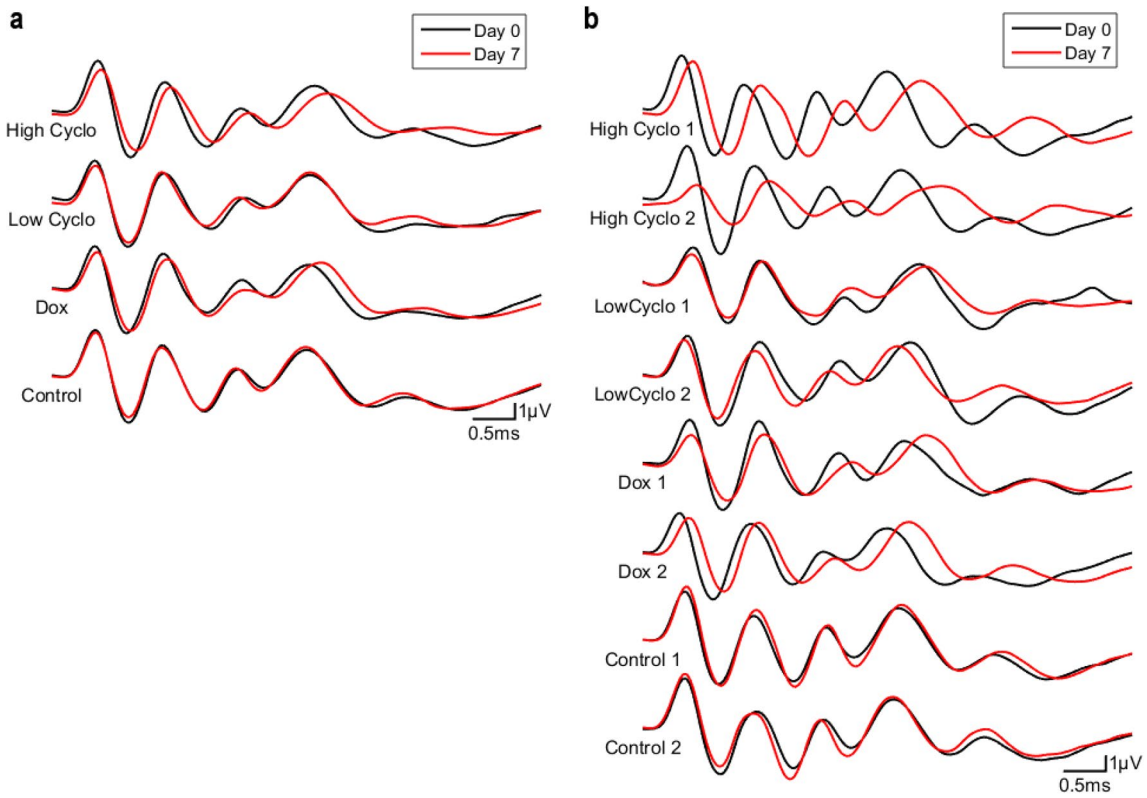

Fig. 5 Average ABR waveforms for each group (**a**) and two individual animals in each treatment group (**b**) (collapsed over 60, 70, and 80 dB pSPL) at day 0 and day 7

treated animals as well. Waveforms from control and low dose cyclophosphamide animals do not demonstrate these features corresponding to the lack of a significant difference at day 7 in the low dose cyclophosphamide treatment group.

To gain a more detailed understanding of the P1–P5 interpeak latency changes across the groups, we assessed latency change for P1 and change in interpeak latency for P1–P2, P2–P3, P3–P4, and P4–P5.

Change in P1 latency

Change in P1 latency was assessed with a three-factor mixed-design ANOVA [Treatment × Time x Sound Level] with treatment as a between-subjects factor, and time and sound level as within-subjects factors. Results indicated a significant main effect of time ($F_{2.4, 84.5} = 26.269$; $p < 0.001$, $\eta_p^2 = 0.429$, Greenhouse–Geisser corrected). This main effect was qualified by a significant interaction between treatment and time ($F_{7.2, 84.5} = 2.314$; $p = 0.031$, $\eta_p^2 = 0.165$, Greenhouse–Geisser corrected).

Given that there was a time by treatment interaction and no time by treatment by sound level interaction, data were collapsed across sound level (see Fig. 4b). Simple effect analysis of the interaction between treatment and time revealed a significant difference in the P1 latency change among the treatment groups on day 7 ($F_{3, 35} = 3.899$; $p = 0.017$, $\eta_p^2 = 0.250$) and day 14 ($F_{3, 35} = 3.232$; $p = 0.034$, $\eta_p^2 = 0.217$). Follow-up pairwise comparisons utilizing Fisher's LSD indicated that the high dose cyclophosphamide group had a significant increase in P1 latency compared to both the low dose cyclophosphamide group and the control group on days 7 and 14 (p's < 0.042). Although no group differences were significant via the simple effect analysis on days 1 and 56, the pattern was similar to the pattern on days 7 and 14 in that the high dose cyclophosphamide group had the largest P1 latency increase on days 1 and 56 as well.

Change in P1–P2 interpeak latency

Change in P1–P2 interpeak latency was assessed with a three-factor mixed-design ANOVA [Treatment × Time x Sound Level] with treatment as a between-subjects factor, and time and sound level as within-subjects factors. Results indicated significant main effects of both time ($F_{4, 140} = 5.136$; $p < 0.001$, $\eta_p^2 = 0.128$) and of sound level ($F_{2, 70} = 9.459$; $p < 0.001$, $\eta_p^2 = 0.213$). The main effect of time was qualified by a significant interaction between treatment and time ($F_{12, 140} = 2.778$; $p = 0.002$, $\eta_p^2 = 0.192$). The main effect of time and the main effect of sound level was modified by an interaction between the two

($F_{5.1, 178.8} = 5.254$; $p < 0.002$, $\eta_p^2 = 0.131$, Greenhouse–Geisser corrected).

Simple effect analysis to explore the time by sound level interaction revealed a significant difference in P1–P2 interpeak latency change across time at 60 ($F_{4, 38} = 10.585$; $p < 0.001$, $\eta_p^2 = 0.218$) and at 70 dB pSPL ($F_{4, 38} = 4.177$; $p < 0.003$, $\eta_p^2 = 0.099$). Follow-up pairwise comparisons utilizing Fisher's LSD indicated that P1–P2 interpeak latency change was larger at 6 months than at any other timepoint at 60 dB pSPL (p's < 0.001) and that it was larger at 6 months than on days 1, 14, and 56 at 70 dB pSPL (p's < 0.01).

Given that there was a time by treatment interaction and no time by treatment by sound level interaction, data were collapsed across sound level (see Fig. 4c). Simple effect analysis of the interaction between treatment and time revealed a significant difference in P1–P2 interpeak latency change among the treatment groups on day 7 ($F_{3, 35} = 5.453$; $p = 0.003$, $\eta_p^2 = 0.319$) and day 56 ($F_{3, 35} = 2.912$; $p = 0.048$, $\eta_p^2 = 0.200$). Follow-up pairwise comparisons utilizing Fisher's LSD indicated that on day 7 the high dose cyclophosphamide and doxorubicin treatment groups had significant increases in P1–P2 interpeak latency compared to both the low dose cyclophosphamide and control groups (p's < 0.05). However, at day 56, high dose cyclophosphamide treated animals had significant decreases in P1–P2 interpeak latency compared to both doxorubicin and low dose cyclophosphamide groups (p's < 0.02). In addition, there was a trend toward a difference compared to the control group ($p = 0.06$).

Change in P2–P3 interpeak latency

Change in P2–P3 interpeak was assessed with a three-factor mixed-design ANOVA [Treatment × Time x Sound Level] with treatment as a between-subjects factor, and time and sound level as within-subjects factors. Results indicated a significant main effect of treatment ($F_{3, 35} = 6.466$; $p = 0.001$, $\eta_p^2 = 0.357$) and of time ($F_{3.2, 110.7} = 7.348$; $p < 0.001$, $\eta_p^2 = 0.174$, Greenhouse–Geisser corrected). The main effect of time was qualified by a significant interaction between time and sound level ($F_{5.2, 182.4} = 2.465$; $p = 0.032$, $\eta_p^2 = 0.066$, Greenhouse–Geisser corrected).

Simple effect analysis to explore the time by sound level interaction revealed a significant difference in P2–P3 interpeak latency change across time at 60 ($F_{4, 38} = 10.747$; $p < 0.001$, $\eta_p^2 = 0.220$) and at 70 dB pSPL ($F_{4, 38} = 10.797$; $p < 0.001$, $\eta_p^2 = 0.221$). Follow-up pairwise comparisons utilizing Fisher's LSD indicated that P2–P3 interpeak latency change was larger at 6 months than at any other time at 60 dB (p's < 0.002) and that it was larger at 6 months than on days 1, 14, and 56 at 70 dB (p's < 0.002), the same pattern as seen for the time by sound level interaction for P1–P2. In short, when threshold has increased the most relative to the baseline recording (day 0), the interpeak latencies change less at the higher sound-levels.

Follow-up pairwise comparison using Fisher's LSD to investigate the significant main effect of treatment indicated that the P2–P3 interpeak latency change was significantly greater, overall, in the high dose cyclophosphamide group compared to all other treatment groups (p's < 0.03). As expected, given that there was no time by treatment interaction, the P2–P3 interpeak latency change is more positive (greater increase days 1–56 and less of a decrease at 6 months) for the high dose cyclophosphamide group at all timepoints compared to all the other groups (see Fig. 4d). However, this difference between the high dose cyclophosphamide group and all the other groups appears to be driven by a slowing of the P2–P3 interpeak latency by the other groups at 6 months, whereas the difference appears to be driven by an increase in the P2–P3 interpeak latency in the high cyclophosphamide group on the earlier days.

Change in P3–P4 interpeak latency

Change in P3–P4 interpeak latency was assessed with a three-factor mixed-design ANOVA [Treatment × Time x Sound Level] with treatment as a between-subjects factor, and time and sound level as within-subjects factors. Results indicated a significant main effect of time ($F_{2.9, 99.8} = 9.491$; $p < 0.001$, $\eta_p^2 = 0.213$, Greenhouse–Geisser corrected) and of sound level ($F_{2, 70} = 3.432$; $p = 0.038$, $\eta_p^2 = 0.089$). The main effect of time was qualified by a significant interaction between treatment and time ($F_{8.6, 99.8} = 3.001$; $p < 0.004$, $\eta_p^2 = 0.205$, Greenhouse–Geisser corrected).

Follow-up pairwise comparisons utilizing Fisher's LSD indicated that P3–P4 interpeak latency change was larger at 80 than at 60 dB pSPL ($p = 0.017$).

Given that there was a time by treatment interaction and no treatment by time by sound level interaction, data were collapsed across sound level (see Fig. 4e). Simple effect analysis of the interaction between treatment and time revealed a significant difference in P3–P4 interpeak latency change among the treatment groups on day 14 ($F_{3, 35} = 3.112$; $p = 0.039$, $\eta_p^2 = 0.211$). Follow-up pairwise comparisons utilizing Fisher's LSD indicated that the low dose cyclophosphamide group had a significant decrease in P3–P4 interpeak latency compared to both the high dose cyclophosphamide group and the doxorubicin group (p's < 0.05).

Change in P4–P5 Interpeak latency

Change in P4–P5 interpeak latency was assessed with a three-factor mixed-design ANOVA [Treatment × Time x Sound Level] with treatment as a between-subjects factor, and time and sound level as within-subjects factors. Results indicated a significant main effect of

treatment ($F_{3,\ 35} = 3.160$; $p = 0.037$, $\eta_p^2 = 0.213$), of time ($F_{4,\ 140} = 2.48$; $p = 0.047$, $\eta_p^2 = 0.066$), and of sound level ($F_{1.7,\ 58.7} = 7.572$; $p = 0.002$, $\eta_p^2 = 0.178$, Greenhouse–Geisser corrected). There was a trend ($F_{12,\ 140} = 1.728$; $p = 0.067$, $\eta_p^2 = 0.129$) toward a time by treatment interaction.

Follow-up pairwise comparisons utilizing Fisher's LSD indicated that P4–P5 interpeak latency change became smaller as the sound level increased: overall, latency change was greater at 60 and 70 than at 80 dB pSPL (p's < 0.02).

Follow-up pairwise comparison using Fisher's LSD to investigate the significant main effect of treatment revealed increased P4–P5 interpeak latency changes for high dose cyclophosphamide treated animals compared to all other treatment groups (p's < 0.03). While the high dose cyclophosphamide groups P4–P5 interpeak latency increase was numerically larger than the other groups at all timepoints (see Fig. 4f), this overall difference in P4–P5 interpeak latency appears to be predominantly driven by an increase in P4–P5 interpeak latency in the high dose cyclophosphamide group on days 1, 7, and 14, consistent with the finding of a trend toward a treatment by time interaction.

Although exploratory, simple effect analysis of the time by treatment interaction trend revealed that that there were only differences between the treatment groups on days 1 ($F_{3,\ 35} = 4.58$; $p = 0.008$, $\eta_p^2 = 0.282$), 7 ($F_{3,\ 35} = 7.106$; $p < 0.001$, $\eta_p^2 = 0.379$), and 14 ($F_{3,\ 35} = 5.793$; $p = 0.003$, $\eta_p^2 = 0.332$), and not day 56 ($F_{3,\ 35} = 0.381$; $p = 0.767$, $\eta_p^2 = 0.032$) and 6 months ($F_{3,\ 35} = 0.492$; $p = 0.731$, $\eta_p^2 = 0.036$), consistent with the idea that the overall increase in P4–P5 interpeak latency in the high dose cyclophosphamide group is predominantly driven by the increased interpeak latency on days 1, 7, and 14.

ABR peak amplitude

Figure 6 shows the change in peak amplitude (P1, P2, P3, P4, and P5) relative to baseline recordings, averaged across sound level (60, 70, and 80 dB pSPL).

Change in P1 amplitude

Change in P1 amplitude was assessed with a three-factor mixed-design ANOVA [Treatment × Time × Sound Level] with treatment as a between-subjects factor, and time and sound level as within-subjects factors. Results indicated a significant main effect of time ($F_{3.1,\ 107.9} = 109.537$; $p < 0.001$, $\eta_p^2 = 0.758$, Greenhouse–Geisser corrected).

Figure 6a shows the general pattern of P1 amplitude decreasing over time and that there was little evidence that P1 amplitude varied by treatment.

Change in P2 amplitude

Change in Peak 2 amplitude was assessed with a three-factor mixed-design ANOVA [Treatment × Time × Sound Level] with treatment as a between-subjects factor, and time and sound level as within-subjects factors. Results indicated a significant main effect of time ($F_{3.2,\ 111.7} = 65.999$; $p < 0.001$, $\eta_p^2 = 0.653$, Greenhouse–Geisser corrected) and sound level ($F_{1.6,\ 55.7} = 3.451$; $p = 0.049$, $\eta_p^2 = 0.090$, Greenhouse–Geisser corrected). The main effect of time was qualified by a significant interaction with treatment ($F_{9.6,\ 111.7} = 4.708$; $p < 0.001$, $\eta_p^2 = 0.288$, Greenhouse–Geisser corrected). The main effect of time was also qualified by a significant interaction with sound level ($F_{5.4,\ 189.9} = 5.594$; $p < 0.001$, $\eta_p^2 = 0.138$, Greenhouse–Geisser corrected).

Given that there was a time by treatment interaction and no time by treatment by sound level interaction, data were collapsed across sound level (see Fig. 6b). Simple effect analysis of the interaction between treatment and time revealed a significant difference in the P2 amplitude change among the treatment groups at 6 months ($F_{3,\ 35} = 2.936$; $p = 0.047$, $\eta_p^2 = 0.201$). Follow-up pairwise comparisons utilizing Fisher's LSD indicated that the low dose cyclophosphamide group had a significant decrease in P2 amplitude compared to the high dose cyclophosphamide group ($p = 0.009$) and a trend toward a decrease compared to the control group ($p = 0.053$).

Change in P3 amplitude

Change in Peak 3 amplitude was assessed with a three-factor mixed-design ANOVA [Treatment × Time × Sound Level] with treatment as a between-subjects factor, and time and sound level as within-subjects factors. Results indicated a significant main effect of time ($F_{2.3,\ 80.7} = 17.437$; $p < 0.001$, $\eta_p^2 = 0.333$, Greenhouse–Geisser corrected) which was qualified by a significant interaction with treatment ($F_{6.9,\ 80.7} = 2.709$; $p = 0.015$, $\eta_p^2 = 0.188$, Greenhouse–Geisser corrected).

Given that there was a time by treatment interaction and no time by treatment by sound level interaction, data were collapsed across sound level (see Fig. 6c). Simple effect analysis of the interaction between treatment and time revealed a significant difference in the P3 amplitude change among the treatment groups at 6 months ($F_{3,\ 35} = 5.259$; $p = 0.004$, $\eta_p^2 = 0.311$). Follow-up pairwise comparisons utilizing Fisher's LSD indicated that

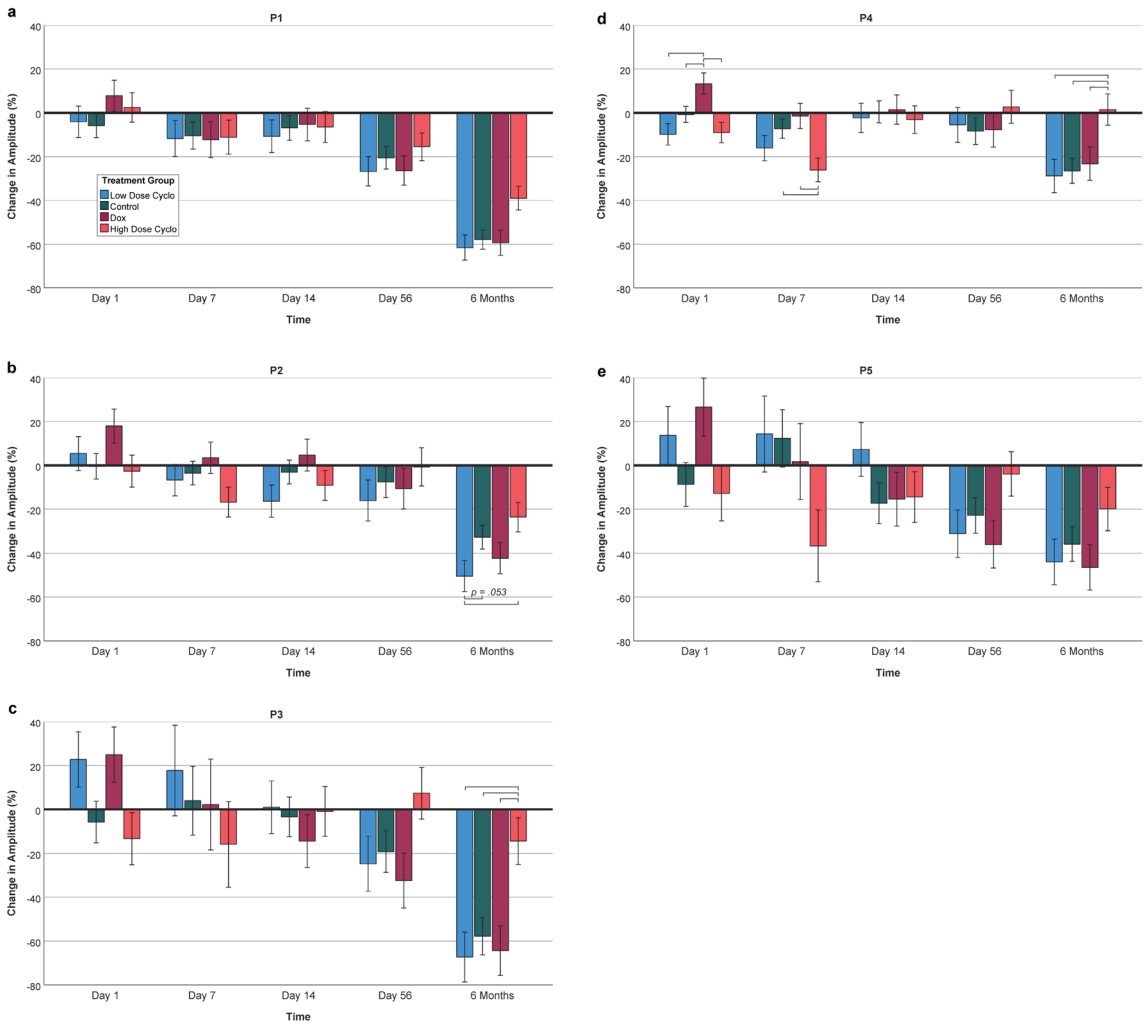

Fig. 6 Percent change in peak amplitude relative to baseline collapsing across sound level. Baseline ABR recordings were performed for each animal 2 days before initiation of chemotherapy administration. After completion of chemotherapy administration, follow-up ABR tests were conducted on each animal at various points during a time course of 6 months. Low dose cyclophosphamide (120 mg/kg) and doxorubicin (5 mg/kg) both consisted of $n = 8$ animals, the high dose cyclophosphamide (220 mg/kg) treatment group consisted of $n = 9$ animals, and the control group consisted of $n = 14$ animals. ABR amplitudes were analyzed for each individual at each timepoint. Change of peak amplitude was calculated as $(A_t–A_0)/A_0$ (A_t, amplitude at day 1, day 7, day 14, day 56, or 6-month post-treatment; A_0, baseline value 2 days before initiation of chemotherapy administration). The mean change in amplitude was averaged across sound level (60, 70, and 80 dB pSPL) for (a) P1, (b) P2, (c) P3, (d) P4, (e) P5. Data represent percent change of amplitude ± S.E.M. Brackets represent significant (p's < 0.05) Fisher's LSD pairwise comparisons

amplitude decreased less for the high dose cyclophosphamide group compared to all other groups (p's < 0.005).

Change in P4 amplitude

Change in Peak 4 amplitude was assessed with a three-factor mixed-design ANOVA [Treatment × Time x Sound Level] with treatment as a between-subjects factor, and time and sound level as within-subjects factors. Results indicated a significant main effect of time ($F_{2.6, 89.7} = 12.544$; $p < 0.001$, $\eta_p^2 = 0.264$, Greenhouse–Geisser corrected) which was qualified by a significant interaction with treatment ($F_{7.7, 89.7} = 4.75$; $p < 0.001$, $\eta_p^2 = 0.289$, Greenhouse–Geisser corrected).

Given that there was a time by treatment interaction and no time by treatment by sound level interaction, data were collapsed across sound level (see Fig. 6d). Simple effect analysis of the interaction between treatment and time revealed a significant difference in the P4 amplitude change among the treatment groups on day 1 ($F_{3, 35} = 4.919$; $p = 0.006$, $\eta_p^2 = 0.297$), day 7 ($F_{3, 35} = 3.937$; $p = 0.016$, $\eta_p^2 = 0.252$) and at 6 months ($F_{3, 35} = 3.955$; $p = 0.016$, $\eta_p^2 = 0.253$). Follow-up pairwise comparisons utilizing Fisher's LSD indicated that on day 1, the doxorubicin group was

significantly different than the other groups (p's < 0.03). On day 7, the high dose cyclophosphamide group had a greater decrease in P4 amplitude than the control and doxorubicin groups (p's < 0.02). At 6 months, the low dose cyclophosphamide, the doxorubicin, and the control group all had a larger reduction in P4 amplitude than the high dose cyclophosphamide group (p's < 0.03).

Change in P5 amplitude

Change in P5 amplitude was assessed with a three-factor mixed-design ANOVA [Treatment × Time x Sound Level] with treatment as a between-subjects factor, and time and sound level as within-subjects factors. Results indicated a significant main effect of time ($F_{2.8, 96.7} = 14.572$; $p < 0.001$, $\eta_p^2 = 0.294$, Greenhouse–Geisser corrected) which was qualified by a significant interaction with treatment ($F_{8.3, 96.7} = 4.25$; $p < 0.001$, $\eta_p^2 = 0.267$, Greenhouse–Geisser corrected).

Simple effect analysis of the interaction between treatment and time revealed no significant difference in P5 amplitude change across groups at any timepoint. Thus, the significant time by treatment interaction indicates that the pattern of P5 amplitude change over time was different for at least some of the groups; however, no group significantly differed from another on any given day. For example, for the low dose cyclophosphamide group, P5 amplitude did not change much over days 1, 7, and 14, and then decreased at day 56 and 6 months; however, for the high dose cyclophosphamide group, P5 amplitude appears to have decreased slightly at all timepoints. The within group pattern differences driving the time by treatment interaction were not analyzed.

Discussion

The results indicate that the doxorubicin and high dose cyclophosphamide regimens caused a decrease in P1–P5 interpeak latency, however, that delay was transient, occurring only on days 1, 7 and 14 for the high dose cyclophosphamide group and only on day 7 for the doxorubicin group. A finer grained analysis indicated that the delay likely has both peripheral and central origins. The decrease in P1 latency on days 7 and 14 in the high dose cyclophosphamide group suggests that at least part of the impairment is peripheral. The increased P2–P3 and P4–P5 interpeak latencies in the high dose cyclophosphamide group suggests that the high dose cyclophosphamide animals had a transient central impairment.

Overall, there were few differences in amplitude between the control group and any of the treatment groups. For P2, there was a trend toward a greater decrease in amplitude for the low dose cyclophosphamide group at 6 months compared to the control group. For P4, there was a greater decrease in amplitude for the high dose cyclophosphamide at day 7 compared to the control group. Surprisingly, at 6 months, the P3 and P4 amplitude decreased less in the high dose cyclophosphamide group compared to the control group. Interestingly, although not statistically significant, this pattern of a smaller decrease in amplitude in the high dose cyclophosphamide group at 6 months is seen for all the peaks. It is unclear why that would be. A decrease in the peak amplitudes at 6 months is expected as the hearing threshold increases: in our data, we saw about a 6 dB change in threshold level between the day 0 recordings and the recordings at 6 months. Thus, if the high dose cyclophosphamide group's hearing threshold was lower at 6 months than the other groups, that could explain the difference; however, there were no differences in threshold among the groups at 6 months.

There was little evidence that animals exposed to a low dose of cyclophosphamide had an impaired ABR. In fact, at day 14 the P1–P5 latency and P3–P4 latency decreased relative to the control group. This finding may be related to the fact that, in addition to its cytotoxic properties, cyclophosphamide has both anti-inflammatory and immunosuppressive effects, and in some cases, is even used to treat central nervous system inflammation in multiple sclerosis (Weiner and Cohen 2002). We had hypothesized that treatment with doxorubicin or cyclophosphamide might cause changes in the ABR waveform, and more specifically, that it might cause both a reduction in transmission speed and a reduction in amplitude indicative of myelin damage. We found changes in transmission speed at what appears to be peripheral and central levels; however, they were transient. We did not see any across the board decreases in amplitude indicative of widespread myelin damage. The amplitude changes we did see suggest a central mechanism. The ABR waveform as a whole, as well as individual peaks, likely represent the activity of parallel pathways and the firing of multiple cell types (e.g., Land et al. (2016); Melcher & Kiang (1996)) making the identification of any specific structure as being damaged difficult. In fact, the damage may not even be early in the auditory processing stream as damage to the auditory cortex can cause changes to the ABR (Lamas et al. 2013).

As discussed earlier, Han et al. (2008) observed increased ABR interpeak latencies in mice treated with 5-FU up to 56-day post-treatment and also detected reduced cellularity within the corpus callosum 6-month post-treatment. Here we found increased interpeak latencies in mice treated with doxorubicin and also in mice treated with cyclophosphamide; however, in the present experiment, the impairment was not apparent by day 56. It may be the case that specific chemotherapy compounds and dosage lead to longer or shorter lasting changes to the ABR. Further investigation should aim to replicate the long-term ABR impairment seen with 5-FU. In addition, it will be important to explore

how various combinations of chemotherapy agents affect the ABR. Cancer treatment is typically via a combination of chemotherapy agents and such combinations may cause larger or longer lasting changes.

The transient nature of the ABR impairments detected in the current study stress the importance of investigating CRCI across greater time intervals. Reviews by Both Evenden (2013) and Seigers and Fardell (2011) highlight that a key difference between the human and the animal literature concerning CRCI is the time course of assessment and the duration of cognitive impairments examined. Clinical studies often assess CRCI across months to years, while animal studies typically examine CRCI across days to weeks. While understanding the underlying mechanisms and impact of transient CRCI is important, further investigation of long-term effects within the animal literature is needed, especially when clinical studies suggest that for many, but not all, CRCI following chemotherapy treatment seems to ameliorate gradually within 1–2 years (Billiet et al. 2018; erulla et al. 2020).

The nature of the transient impairment seen here is unclear. It is conceivable that the impairment reflects moderate and perhaps sporadic myelin damage. Another possibility is that neuroinflammatory processes may be responsible for the ABR changes detected within the first few weeks following chemotherapy treatment. Several studies have detected upregulation of pro-inflammatory mediators (such as CD68, COX-2, ED-1, IL-6, IL-1β, TNF-α) following chemotherapy, in both the animal and clinical literature (For a review see McLeary et al. 2019). Furthermore, Briones and Woods (2014) have demonstrated that rats treated with CMF (drug combination of cyclophosphamide, methotrexate, and 5-fluorouracil) show increased levels of inflammatory mediators, that accompany both cognitive impairment and myelin abnormalities, which were detected up to 4 weeks following treatment. In addition, while not often explored in the animal literature, fatigue is a commonly reported side effect of chemotherapy (Bower 2014) and pro-inflammatory processes have been suggested as a possible mechanism (Liu et al. 2012; Weymann et al. 2014). Thus, neuroinflammation and fatigue may play a role in the transient increases in interpeak latency and decreases in amplitude detected predominantly in the high cyclophosphamide group.

The choice of mouse strain may also have played a role in our results. C57BL/6 J mice develop early presbycusis (Keithley et. al. 2004; Hunter and Willott 1987); however, it is unclear the degree to which this tendency would make C57BL/6Js more or less susceptible to detectable chemotherapy-related ABR changes. We also note that click stimuli were used in the present study. It is possible that different frequencies and corresponding processing may be more or less susceptible to chemotherapy induced impairment and that this susceptibility may change with age.

In summary, our results suggest that i.p. injections of doxorubicin and high dose cyclophosphamide seem to cause transient impairments in the ABR of mice, and that the extent and time course of the changes may differ based on chemotherapy compound and dose. The changes seemed to occur more consistently and over a longer time period in the high dose cyclophosphamide treated animals than in the doxorubicin treated animals. It is important to note that while the treatment animals experienced significant weight-loss, it is possible that a higher dose of cyclophosphamide or doxorubicin might have resulted in a longer lasting change in the ABR. The current results provide evidence that ABR analysis may be a useful tool for identifying and screening individuals for early signs of cognitive sequelae that may be at risk for developing CRCI, and may be one avenue to bridge the gap between human and animal models. Further investigation should determine to what degree ABR analysis might help detect long-term changes to myelin integrity or other neural targets and the degree to which these effects may be associated with particular chemotherapeutic compounds or combinations of compounds.

Funding This study was funded in part by DOD grant (W81XWH-10–1-0692).

Data availability The data sets generated during and/or analyzed during the current study are available from the corresponding author on reasonable request.

Declarations

Conflict of interest The authors have no competing interests to declare that are relevant to the content of this article.

References

Ahles TA, Saykin AJ (2007) Candidate mechanisms for chemotherapy-induced cognitive changes. Nat Rev Cancer 7:192–201. https://doi.org/10.1038/nrc2073

Billiet T, Emsell L, Vandenbulcke M et al (2018) Recovery from chemotherapy-induced white matter changes in young breast cancer survivors? Brain Imaging Behav 12:64–77. https://doi.org/10.1007/s11682-016-9665-8

Bower JE (2014) Cancer-related fatigue—mechanisms, risk factors, and treatments. Nat Rev Clin Oncol 11:597

Briones TL, Woods J (2014) Dysregulation in myelination mediated by persistent neuroinflammation: possible mechanisms in chemotherapy-related cognitive impairment. Brain Behav Immun 35:23–32. https://doi.org/10.1016/j.bbi.2013.07.175

Briones TL, Woods J (2011) Chemotherapy-induced cognitive impairment is associated with decreases in cell proliferation and histone modifications. BMC Neurosci 12:1–13. https://doi.org/10.1186/1471-2202-12-124

Brismar T (1981) Electrical properties of isolated demyelinated rat nerve fibers. Acta Physiol Scand 113:161–166. https://doi.org/10.1111/j.1748-1716.1981.tb06877.x

Burkard R (2006) Calibration of acoustic transients. Brain Res 1091:27–31. https://doi.org/10.1016/j.brainres.2006.02.132

Carpinelli MR, Voss AK, Manning MG et al (2014) A new mouse model of Canavan leukodystrophy displays hearing impairment due to central nervous system dysmyelination. Dis Model Mech 7(6):649–657. https://doi.org/10.1242/dmm.014605

Christie LA, Acharya MM, Parihar VK et al (2012) Impaired cognitive function and hippocampal neurogenesis following cancer chemotherapy. Clin Cancer Res 18:1954–1965. https://doi.org/10.1158/1078-0432.CCR-11-2000

Collins B, MacKenzie J, Tasca GA et al (2014) Persistent cognitive changes in breast cancer patients 1 year following completion of chemotherapy. J Int Neuropsychol Soc 20:370–379. https://doi.org/10.1017/s1355617713001215

Cragg BG, Thomas PK (1964) Changes in nerve conduction in experimental allergic neuritis. J Neurol Neurosurg Psychiatry 27:106–115. https://doi.org/10.1136/jnnp.27.2.106

Cerulla TN, Navarro Pastor JB, de Chaparrola Osa N (2020) Systematic review of cognitive sequelae of non-central nervous system cancer and cancer therapy. J Cancer Surv 14:1–19. https://doi.org/10.1007/s11764-020-00870-2

Evenden J (2013) Cognitive impairments and cancer chemotherapy: translational research at a crossroads. Life Sci 93:589–595. https://doi.org/10.1016/j.lfs.2013.03.020

Focan C (1995) Circadian rhythms and cancer chemotherapy. Pharmacol Ther 67:1–52. https://doi.org/10.1016/0163-7258(95)00009-6

Foley JJ, Raffa RB, Walker EA (2008) Effects of chemotherapeutic agents 5-fluorouracil and methotrexate alone and combined in a mouse model of learning and memory. Psychopharmacology 199:527–538. https://doi.org/10.1007/s00213-008-1175-y

Fremouw T, Fessler CL, Ferguson RJ, Burguete Y (2012a) Preserved learning and memory in mice following chemotherapy: 5-Fluorouracil and doxorubicin single agent treatment, doxorubicin–cyclophosphamide combination treatment. Behav Brain Res 226:154–162. https://doi.org/10.1016/j.bbr.2011.09.013

Fremouw T, Fessler CL, Ferguson RJ, Burguete Y (2012b) Recent and remote spatial memory in mice treated with cytosine arabinoside. Pharmacol Biochem Behav 100:451–457. https://doi.org/10.1016/j.pbb.2011.10.008

Gandal MJ, Ehrlichman RS, Rudnick ND, Siegel SJ (2008) A novel electrophysiological model of chemotherapy-induced cognitive impairments in mice. Neuroscience 157:95–104. https://doi.org/10.1016/j.neuroscience.2008.08.060

Geraghty AC, Gibson EM, Ghanem RA et al (2019) Loss of adaptive myelination contributes to methotrexate chemotherapy-related cognitive impairment. Neuron 103:250–265. https://doi.org/10.1016/j.neuron.2019.04.032

Han R, Yang YM, Dietrich J et al (2008) Systemic 5-fluorouracil treatment causes a syndrome of delayed myelin destruction in the central nervous system. J Biol 7:12.1-12.22

Henry KR (1979) Auditory brainstem volume-conducted responses: origins in the laboratory mouse. J Am Audit Soc 4:173–178

Hunter KP, Willott JF (1987) Aging and the auditory brainstem response in mice with severe or minimal presbycusis. Hear Res 30:207–218. https://doi.org/10.1016/0378-5955(87)90137-7

Janelsins MC, Heckler CE, Peppone LJ et al (2018) Longitudinal trajectory and characterization of cancer-related cognitive impairment in a nationwide cohort study. J Clin Oncol 36:3231–3239

Janelsins MC, Roscoe JA, Berg MJ et al (2010) IGF-1 partially restores chemotherapy-induced reductions in neural cell proliferation in adult C57BL/6 mice. Cancer Invest 28:544–553. https://doi.org/10.3109/07357900903405942

Jerger J, Hall J (1980) Effects of age and sex on auditory brainstem response. Arch Otolaryngol 106:387–391. https://doi.org/10.1001/archotol.1980.00790310011003

Keithley EM, Canto C, Zheng QY et al (2004) Age-related hearing loss and the ahl locus in mice. Hear Res 188:21–28. https://doi.org/10.1016/s0378-5955(03)00365-4

Koppelmans V, Breteler MMB, Boogerd W et al (2012) Neuropsychological performance in survivors of breast cancer more than 20 years after adjuvant chemotherapy. J Clin Oncol 30:1080–1086. https://doi.org/10.1200/JCO.2011.37.0189

Lamas V, Alvarado JC, Carro J, Merchán MA (2013) Long-Term Evolution of Brainstem Electrical Evoked Responses to Sound after Restricted Ablation of the Auditory Cortex. PLoS ONE 8(9):e73585. https://doi.org/10.1371/journal.pone.0073585

Land R, Burghard A, Kral A (2016) The contribution of inferior colliculus activit to the auditory brainstem response in mice. Hear Res 341:109–118. https://doi.org/10.1016/j.heares.2016.08.008

Liu L, Mills PJ, Rissling M et al (2012) Fatigue and sleep quality are associated with changes in inflammatory markers in breast cancer patients undergoing chemotherapy. Brain Behav Immun 26:706–713. https://doi.org/10.1016/j.bbi.2012.02.001

Long JM, Lee GD, Kelley-Bell B et al (2011) Preserved learning and memory following 5-fluorouracil and cyclophosphamide treatment in rats. Pharmacol Biochem Behav 100:205–211. https://doi.org/10.1016/j.pbb.2011.08.012

Long P, Wan G, Roberts MT, Corfas G (2018) Myelin development, plasticity, and pathology in the auditory system. Develop Neurobiol. 78:80–92

MacLeod JE, DeLeo JA, Hickey WF et al (2007) Cancer chemotherapy impairs contextual but not cue-specific fear memory. Behav Brain Res 181:168–172. https://doi.org/10.1016/j.bbr.2007.04.003

Martin BA, Tremblay KL, Stapells DR (2007) Principles and applications of cortical auditory evoked potentials. In: Eggermont JJ, Don M (eds) Burkard RF. Auditory Evoked Potentials: Basic Principles and Clinical Applications. Lippincott Williams & Wilkins, Philadelphia, pp 482–507

Matsos A, Johnston IN (2019) Chemotherapy-induced cognitive impairments: a systematic review of the animal literature. Neurosci Biobehav Rev 102:382–399. https://doi.org/10.1016/j.neubiorev.2019.05.001

Matsos A, Loomes M, Zhou I et al (2017) Chemotherapy-induced cognitive impairments: white matter pathologies. Cancer Treat Rev 61:6–14. https://doi.org/10.1016/j.ctrv.2017.09.010

McLeary F, Davis A, Rudrawar S et al (2019) Mechanisms underlying select chemotherapeutic-agent-induced neuroinflammation and subsequent neurodegeneration. Eur J Pharmacol 842:49–56. https://doi.org/10.1016/j.ejphar.2018.09.034

Melcher JR, Kiang NY (1996) Generators of the brainstem auditory evoked potential in cat. III: Identified cell populations. Hear Res 93(1–2):52–71. https://doi.org/10.1016/0378-5955(95)00200-6. PMID: 8735068

Miller KD, Nogueira L, Mariotto AB et al (2019) Cancer treatment and survivorship statistics, 2019. CA Cancer J Clin 69:363–385

Naito R, Murofushi T, Mizutani M, Kaga K (1999) Auditory brainstem responses, electrocochleograms, and cochlear microphonics in the myelin deficient mutant hamster 'bt.' Hear Res 136:44–48. https://doi.org/10.1016/S0378-5955(99)00107-0

Ogier M, Andéol G, Sagui E, Dal Bo G (2020) How to detect and track chronic neurologic sequelae of COVID-19? Use of auditory brainstem responses and neuroimaging for long-term patient follow-up. Brain Behav Immunity-Health 5:100081. https://doi.org/10.1016/j.bbih.2020.100081

Parham K, Sun XM, Kim DO (2001) Noninvasive assessment of auditory function in mice: Auditory brainstem response and distortion product otoacoustic emissions. In: Willott JF (ed) Handbook of Mouse Auditory Research: From Behavior to Molecular Biology. CRC Press, New York, pp 37–58

Raffa RB, Tallarida RJ (2010) Chemo fog: cancer chemotherapy-related cognitive impairment. Preface. Adv Exp Med Biol 678:vii-viii. PMID: 20737998

Reiriz AB, Reolon GK, Preissler T et al (2006) Cancer chemotherapy and cognitive function in rodent models: memory impairment induced by cyclophosphamide in mice. Clin Cancer Res 12:5000–5001. https://doi.org/10.1158/1078-0432.CCR-06-0138

Ren X, Boriero D, Chaiswing L et al (2019) Plausible biochemical mechanisms of chemotherapy-induced cognitive impairment ("chemobrain"), a condition that significantly impairs the quality of life of many cancer survivors. Biochimica Et Biophy Acta Mole Basis Dis 1865:1088–1097. https://doi.org/10.1016/j.bbadis.2019.02.007

Roncagliolo M, Benítez J, Eguibar JR (2000) Progressive deterioration of central components of auditory brainstem responses during postnatal development of the myelin mutant taiep rat. Audiol Neurotol 5:267–275. https://doi.org/10.1159/000013891

Seigers R, Fardell JE (2011) Neurobiological basis of chemotherapy-induced cognitive impairment: a review of rodent research. Neurosci Biobehav Rev 35:729–741. https://doi.org/10.1016/j.neubiorev.2010.09.006

Shah SN, Salamy A (1980) Auditory-evoked far-field potentials in myelin deficient mutant quaking mice. Neuroscience 5:2321–2323. https://doi.org/10.1016/0306-4522(80)90148-7

Vardy J, Rourke S, Tannock IF (2007) Evaluation of cognitive function associated with chemotherapy: a review of published studies and recommendations for future research. J Clin Oncol 25:2455–2463. https://doi.org/10.1200/jco.2006.08.1604

Wan G (2017) Corfas G (2017) Transient auditory nerve demyelination as a new mechanism for hidden hearing loss. Nat Commun 17(8):14487. https://doi.org/10.1038/ncomms14487

Wefel JS, Vardy J, Ahles T, Schagen SB (2011) International cognition and cancer task force recommendations to harmonise studies of cognitive function in patients with cancer. Lancet Oncol 12:703–708. https://doi.org/10.1016/s1470-2045(10)70294-1

Weiner HL, Cohen JA (2002) Treatment of multiple sclerosis with cyclophosphamide: critical review of clinical and immunologic effects. Mult Scler J 8:142–154. https://doi.org/10.1191/1352458502ms790oa

Weiss B (2010) Evaluation of multiple neurotoxic outcomes in cancer chemotherapy. In: Raffa RB, Tallarida RJ (eds) Chemo fog: cancer chemotherapy-related cognitive impairment, vol 678. Springer & Landes, New York, p 96

Weymann KB, Wood LJ, Zhu X, Marks DL (2014) A role for orexin in cytotoxic chemotherapy-induced fatigue. Brain Behav Immun 37:84–94

Winocur G, Henkelman M, Wojtowicz JM et al (2012) The effects of chemotherapy on cognitive function in a mouse model: a prospective study. Clin Cancer Res 18:3112–3121. https://doi.org/10.1158/1078-0432.CCR-12-0060

Winocur G, Johnston I, Castel H (2018) Chemotherapy and cognition: international cognition and cancer task force recommendations for harmonising preclinical research. Cancer Treat Rev 69:72–83. https://doi.org/10.1016/j.ctrv.2018.05.017

Wood LJ, Nail LM, Perrin NA et al (2006) The cancer chemotherapy drug etoposide (VP-16) induces proinflammatory cytokine production and sickness behavior–like symptoms in a mouse model of cancer chemotherapy–related symptoms. Biol Res Nursing 8:157–169

Xing Y, Samuvel DJ, Stevens SM et al (2012) Age-related changes of myelin basic protein in mouse and human auditory nerve. PLoS ONE 7:e34500. https://doi.org/10.1371/journal.pone.0034500

Zheng QY, Johnson KR, Erway LC (1999) Assessment of hearing in 80 inbred strains of mice by ABR threshold analyses. Hear Res 130:94–107. https://doi.org/10.1016/S0378-5955(99)00003-9

Zhou R, Abbas PJ, Assouline JG (1995) Electrically evoked auditory brainstem response in peripherally myelin-deficient mice. Hear Res 88:98–106. https://doi.org/10.1016/0378-5955(95)00105-D